

Research Article

Cite this article: Larrazabal C, Silva LMR, Hermosilla C, Taubert A (2021). Ezetimibe blocks *Toxoplasma gondii*-, *Neospora caninum*- and *Besnoitia besnoiti*-tachyzoite infectivity and replication in primary bovine endothelial host cells. *Parasitology* **148**, 1107–1115. <https://doi.org/10.1017/S0031182021000822>

Received: 12 March 2021
Revised: 23 April 2021
Accepted: 19 May 2021
First published online: 24 May 2021


Key words:

Besnoitia besnoiti; Ezetimibe; *Neospora caninum*; NPC1L1; *Toxoplasma gondii*

Author for correspondence:

Camilo Larrazabal, E-mail: Camilo.Larrazabal@vetmed.uni-giessen.de

Ezetimibe blocks *Toxoplasma gondii*-, *Neospora caninum*- and *Besnoitia besnoiti*-tachyzoite infectivity and replication in primary bovine endothelial host cells

Camilo Larrazabal , Liliana M. R. Silva, Carlos Hermosilla and Anja Taubert

Institute of Parasitology, Biomedical Research Center Seltersberg, Justus Liebig University Giessen, 35392 Giessen, Germany

Abstract

Coccidia are obligate apicomplexan parasites that affect humans and animals. In fast replicating species, *in vitro* merogony takes only 24–48 h. In this context, successful parasite proliferation requires nutrients and other building blocks. Coccidian parasites are auxotrophic for cholesterol, so they need to obtain this molecule from host cells. In humans, ezetimibe has been applied successfully as hypolipidaemic compound, since it reduces intestinal cholesterol absorption *via* blockage of Niemann–Pick C-1 like-1 protein (NPC1L1), a transmembrane protein expressed in enterocytes. To date, few data are available on its potential anti-parasitic effects in primary host cells infected with apicomplexan parasites of human and veterinary importance, such as *Toxoplasma gondii*, *Neospora caninum* and *Besnoitia besnoiti*. Current inhibition experiments show that ezetimibe effectively blocks *T. gondii*, *B. besnoiti* and *N. caninum* tachyzoite infectivity and replication in primary bovine endothelial host cells. Thus, 20 μM ezetimibe blocked parasite proliferation by 73.1–99.2%, *via* marked reduction of the number of tachyzoites per meront, confirmed by 3D-holotomographic analyses. The effects were parasitostatic since withdrawal of the compound led to parasite recovery with resumed proliferation. Ezetimibe-glucuronide, the *in vivo* most effective metabolite, failed to affect parasite proliferation *in vitro*, thereby suggesting that ezetimibe effects might be NPC1L1-independent.

Introduction

Toxoplasma gondii, *Neospora caninum* and *Besnoitia besnoiti* are cyst-forming species belonging to the Apicomplexa phylum, which consists of a large group of obligatory intracellular protozoan parasites that affect both humans and animals. Despite morphological similarities between coccidian species, host specificity and clinical consequences greatly differ among them. In this context, *T. gondii* is considered a major public health problem and an abortive agent especially in ovines (Benavides *et al.*, 2017) and humans (Nayeri *et al.*, 2020). The closely related coccidian parasite *N. caninum* is currently considered as a major cause of abortions in cattle (Reichel *et al.*, 2013). In contrast, *B. besnoiti* causes bovine besnoitiosis, an emerging disease within Europe, which is characterized by massive alterations of skin and mucosae and also bull infertility (Alvarez-Garcia *et al.*, 2013).

During the acute stage of infection, coccidian parasites undergo asexual replication within host cells. In this context, host endothelial cells have shown high permissiveness for tachyzoite infection and proliferation *in vivo* (Alvarez-Garcia *et al.*, 2013; Konradt *et al.*, 2016). Likewise, primary bovine endothelial cells have consistently been reported as suitable for *in vitro* replication of *T. gondii*, *N. caninum* and *B. besnoiti* (Taubert *et al.*, 2006, 2016; Silva *et al.*, 2019; Velásquez *et al.*, 2019), allowing high tachyzoite proliferation rates in an experimental set up close to the *in vivo* scenario. During the fast proliferation phase, tachyzoites need significant amounts of nutrients for offspring development, which may be obtained from the host cell or newly synthesized. Specifically during coccidian replication high amounts of cholesterol are needed for new membrane biosynthesis (Coppens, 2013). Given that apicomplexan parasites are considered auxotrophic for cholesterol (Coppens, 2013), their replication within the parasitophorous vacuole (PV) highly depends on cholesterol supply by the host cell. In general, cellular cholesterol supply may be achieved either by enhancement of cellular endogenous *de novo* biosynthesis or by an increased cholesterol uptake from extracellular sources (Luo *et al.*, 2020). In line, apicomplexan parasites can differentially exploit cholesterol sources depending on host cell type and parasite species. LDL internalization appears the main pathway for cholesterol uptake, and cholesterol esterification allows for storage in lipid-rich organelles (Luo *et al.*, 2020). Recently, LDL-mediated cholesterol incorporation was described as pivotal, but not exclusive mechanism to fulfil cholesterol requirement during fast replicating coccidia proliferation (Nolan *et al.*, 2015; Silva *et al.*, 2019).

Based on pathophysiological consequences of human hyperlipidaemia, several pharmacological lipid-lowering compounds have been developed (Barter and Rye, 2016). Amongst these, ezetimibe is one of the most common hypolipidaemic drugs, which is capable of

reducing intestinal cholesterol absorption by its interaction with Niemann–Pick C-1 like-1 protein (NPC1L1) in enterocytes (Davis *et al.*, 2004; Garcia-Calvo *et al.*, 2005). In detail, ezetimibe binds to NPC1L1, resulting in the blockage of NPC1L1 endocytosis into clathrin-coated vesicles and thereby diminishing cholesterol internalization into enterocytes (Ge *et al.*, 2008; Wang *et al.*, 2009). Despite that, the participation of other potential ezetimibe targets as the class B type 1 scavenger receptor (SR-BI) and the aminopeptidase N (CD13) have been linked to its hypolipidaemic effect (Kramer *et al.*, 2005; Labonté *et al.*, 2007). In general, the efficacy and safety of ezetimibe has been reported in mice and human studies (Bays *et al.*, 2001; van Heek *et al.*, 2001). As such, ezetimibe might represent a promising anti-parasitic drug candidate (Andrade-Neto *et al.*, 2016). In line, ezetimibe treatments significantly reduced *Cryptosporidium parvum* growth in Caco-2 cells (Ehrenman *et al.*, 2013). However, other evidences are incongruent: whilst ezetimibe reduced the parasite burden of *Leishmania amazonensis* *in vivo*, and diminished the *L. infantum* replication *in vitro* and *in vivo* (alone or in binary and ternary combination with miltefosine and itraconazole) (Andrade-Neto *et al.*, 2016, 2021), this treatment did not affect *Plasmodium yoelii* parasitaemia in mice, while reduced the intraerythrocytic proliferation of *P. falciparum* *in vitro* (Kume *et al.*, 2016; Hayakawa *et al.*, 2021), thereby suggesting parasite-specific effects for this compound.

So far, no data are available on the impact of this drug on typical fast replicating coccidian parasites. Therefore, the aim of this study was to evaluate anti-parasitic efficacy of ezetimibe in *T. gondii*, *N. caninum* and *B. besnoiti*-infected primary bovine host endothelial cells.

Materials and methods

Host cell culture

Primary bovine umbilical vein endothelial cells (BUVEC) were isolated as described elsewhere (Taubert *et al.*, 2006). BUVEC were cultured at 37°C and 5% CO₂ atmosphere in modified endothelial cell growth medium (modECGM), by diluting ECGM medium (Promocell®) with M199 (Sigma-Aldrich) at a ratio of 1:3, supplemented with 500 U/mL penicillin (Sigma-Aldrich) and 50 µg/mL streptomycin (Sigma-Aldrich) and 5% FCS (foetal calf serum; Biochrom). BUVEC of less than three passages were used in this study.

Parasites

Toxoplasma gondii (strain RH) and *Neospora caninum* (strain NC-1) tachyzoites were cultivated *in vitro* as described elsewhere (Taubert *et al.*, 2006; Velásquez *et al.*, 2019), by maintaining them at several passages in permanent African green monkey kidney epithelial cells (MARC 145) in Dubelcco's modified eagle medium (DMEM) (Sigma-Aldrich). *Besnoitia besnoiti* (strain Bb Evora04) tachyzoite stages were propagated in Madin–Darby bovine kidney cells (MDBK) (Velásquez *et al.*, 2020) in Roswell Park Memorial Institute (RPMI) medium (Sigma-Aldrich). All culture media were supplemented with 500 U/mL penicillin and 50 µg/mL streptomycin and 5% foetal calf serum (FCS; Sigma-Aldrich). Infected and non-infected cells were cultured at 37°C and 5% CO₂ atmosphere. Vital tachyzoites were collected from supernatants of infected host cells (800 × g; 5 min) and re-suspended in modECGM for further experiments.

For infection rate-related experiments, tachyzoites of each species were pre-incubated in 20 µM ezetimibe for 1 h. After washing in modECGM (800 × g; 5 min), tachyzoites were used for infection experiments.

Treatments of host cells and infections

BUVEC ($n = 5$) were seeded in 12-well plates (Sarstedt) pre-coated with fibronectin (1:400; Sigma-Aldrich). Ezetimibe (Cayman Chemical) and ezetimibe-glucuronide (Santa Cruz Biotechnology) stock solutions were prepared in dimethyl sulphoxide (DMSO; Sigma-Aldrich, 33 mM), diluted in modECGM at 2.5, 5, 10 and 20 µM and administered to fully confluent cell monolayers 48 h before infection. ModECGM with DMSO (0.06%) served as vehicle control. Following pre-treatments, the medium was entirely removed and cells were infected with tachyzoites of *T. gondii*, *B. besnoiti* or *N. caninum* at a multiplicity of infection of 1:5 for 4 h under inhibitor-free conditions. Then, extracellular tachyzoites were removed and fresh medium with inhibitors was re-administered. At 4 h post infection (p. i.), phase-contrast images for infection rate estimation [(infected cells/total cells) × 100] were acquired by an inverted microscope (IX81, Olympus®) equipped with a digital camera (XM10, Olympus®). Tachyzoites present in cell culture supernatants were collected (800 × g; 5 min) at 48 h p. i. and counted in a Neubauer chamber.

Additionally, withdrawal experiments were carried out. Therefore, ezetimibe-containing medium was replaced by control medium at 24 h p. i., and parasite replication was estimated 24 h later ($n = 5$). Finally, further assays were performed to estimate the effect of ezetimibe over time as cells were treated as described above with a daily replacement of medium containing ezetimibe (20 µM) at 24, 48 and 72 h p. i., and tachyzoite proliferation was observed at 48, 72 and 96 h p. i., respectively ($n = 5$).

Live cell 3D holotomographic microscopy to illustrate parasite development

BUVEC were seeded into 35 mm tissue culture µ-dishes (Ibidi®) and cultured (37°C, 5% CO₂) until confluence. Ezetimibe treatment (20 µM) was performed as described above. Thereafter, *T. gondii*, *N. caninum* and *B. besnoiti* tachyzoites were used to infect cell layers (MOI = 3:1). At 24 h p. i., holotomographic images were obtained by using 3D Cell-Explorer-fluo microscope (Nanolive) equipped with a 60 × magnification ($\lambda = 520$ nm, sample exposure 0.2 mW/mm²) and a depth of field of 30 µM. Images were analysed using STEVE software (Nanolive) to obtain refractive index (RI)-based z-stacks (Silva *et al.*, 2019). Additionally, digital staining was applied according to the RI of intracellular tachyzoites. Finally, intracellular meront development was evaluated by counting intra-meront tachyzoites in at least six 3D holotomographic z-stacks of infected host cells (= 50 cells per condition) in presence or absence of ezetimibe (20 µM).

RT-qPCR for relative quantification of NPC1L1 mRNA

BUVEC ($n = 5$) grown in 25 cm² culture tissue flasks (Greiner Bio-One) were infected with *T. gondii*, *N. caninum* or *B. besnoiti* tachyzoites (MOI = 5:1). Infected- and non-infected host cells were processed for total RNA isolation at four different time points after infection (3, 6, 12, 24 h p. i.). Tissue samples from bovine small intestine obtained at a local slaughterhouse were used as positive controls for NPC1L1. For total RNA isolation, the RNeasy kit (Qiagen) was used according to the manufacturer's instructions. Total RNAs were stored at -80°C until further use. In order to remove any genomic DNA leftover, DNA digestion step was performed. Therefore, 1 µg of total RNA was treated with 10 U DNase I (Thermo Scientific) in 1 × DNase reaction buffer (37°C, 30 min). DNase was inactivated by heating the samples (65°C, 10 min). The efficiency of genomic DNA digestion was confirmed by no-RT-controls in each RT-qPCR experiment. cDNA synthesis was performed using the SuperScript IV

(Invitrogen™) according to the manufacturer's instructions. Briefly, for first-strand cDNA synthesis, 1 µg of DNase treated total RNA was added to 0.5 µL of 50 µM oligo(dt), 1 µL of 50 ng/µL random hexamer primer, 1 µL of 10 mM dNTP mix in a total volume of 10 µL. Thereafter, the samples were incubated at 65°C for 5 min and then immediately cooled on ice. Additionally, 4 µL of 5× SSIV buffer, 1 µL 0.1 M DTT, 1 µL RNase free H₂O and 0.5 µL SuperScript IV enzyme were added obtaining a total volume of 20 µL. The samples were incubated at 23°C for 10 min followed by 50°C for 10 min and an 80°C inactivation step for 10 min.

Probes were labelled at the 5'-end with a reporter dye FAM (6-carboxyfluorescein) and at the 3'-end with the quencher dye TAMRA (6-carboxytetramethyl-rhodamine). bNPC1L1 primer sequences were designed as follows: *Bos taurus* NPC1L1 forward 5'-CTTCCCTGATATGTCTTAC-3'; reverse 5'-GACCAGAGATATAAAGGC-3' probe AGCCAGTCAATGAAGTCGTCCA. qPCR amplification was performed on a Rotor-Gene Q Thermocycler (Qiagen) in duplicates in a 10 µL total volume containing 400 nM forward and reverse primers, 200 nM probe, 10 ng cDNA and 5 µL 2× PerfeCTa qPCR FastMix (Quanta Biosciences). The reaction conditions were as follows: 95°C for 10 min, 40 cycles at 95°C for 10 s, 60°C for 15 s and 72°C for 30 s. No-template controls and no-RT reactions were included in each experiment. As reference gene GAPDH was used as previously reported (Taubert *et al.*, 2006; Hamid *et al.*, 2014; Hamid *et al.*, 2015).

Viability assessment

For experiments on parasite viability, 5×10^5 tachyzoites of each parasite species were treated for 1 h with vehicle (DMSO 0.06%) or ezetimibe (20 µM) (37°C, 5% CO₂). Thereafter, viability of tachyzoites was determined by the trypan blue (Sigma-Aldrich®) exclusion staining assay as described elsewhere (Cervantes-Valencia *et al.*, 2019). Non-stained parasites were considered as viable. Additionally, cell viability after compound treatments was assessed by the colorimetric XTT test (Promega®) according to the manufacturer instructions. Briefly, BUVEC seeded in 96-well plate (Greiner) were incubated with DMSO, ezetimibe or ezetimibe-glucuronide (both 20 µM) in a total volume of 50 µL for 72 h. Thereafter, 50 µL of XTT working solution was added, and samples were incubated for 4 h (37°C, 5% CO₂ atmosphere). The resulting formazan product was estimated *via* optical density (OD) measurements at 590 nm and reference filter 620-nm wavelength using Varioskan™ Flash Multimode Reader (Thermo Scientific).

Statistical analysis

For statistical analyses, the statistical software GraphPad® Prism 8 (version 8.4.3.) was used. Data description was performed by presenting arithmetic mean ± standard deviation. In addition, the non-parametric statistical test Mann–Whitney for comparison of two experimental conditions was applied. In cases of three or more conditions, Kruskal–Wallis test was used. Whenever global comparison by Kruskal–Wallis test indicated significance, *post hoc* multiple comparison tests were carried out by Dunn tests to compare test with control conditions. Outcomes of statistical tests were considered to indicate significant differences when $P \leq 0.05$ (significance level).

Results

Ezetimibe treatments effectively block *T. gondii*, *N. caninum* and *B. besnoiti* tachyzoite proliferation

To analyse the effects of ezetimibe on intracellular tachyzoite replication, functional inhibition experiments were performed,

thereby evaluating the number of freshly released tachyzoites at 48 h p. i. from cells pre-treated and exposed to ezetimibe during the intracellular parasite proliferation stage. Overall, ezetimibe treatments significantly inhibited tachyzoite replication of *T. gondii* (10 µM, $P = 0.0397$; 20 µM, $P = 0.0010$; Figure 1A), *N. caninum* (20 µM, $P = 0.0078$; Figure 1B) and *B. besnoiti* (10 µM, $P = 0.0059$; 20 µM, $P < 0.0001$; Figure 1C) in BUVEC in a dose-dependent manner. Overall, the strongest effect of ezetimibe treatments at 20 µM was observed in case of *B. besnoiti* (99.2 ± 0.5% replication reduction), followed by *T. gondii* (95.7 ± 2.3% reduction) and *N. caninum* (73.1 ± 2.8% reduction). In line, phase-contrast microscopy showed an impairment in meront development for *T. gondii*- (Fig. 1A1 and 1A2), *N. caninum*- (Fig. 1B1 and 1B2) and *B. besnoiti*- (Fig. 1C1 and 1C2) infected BUVEC at 24 h p. i. To better visualize ezetimibe-based effects on parasite development, additionally live cell 3D holotomographic microscopy were performed. As illustrated in Fig. 2, treatments with ezetimibe led to reduced meront sizes in *T. gondii*, *N. caninum* and *B. besnoiti* infections (Fig. 2), without apparently affecting the morphology of non-infected host cells (data not shown). Additionally, the number of tachyzoites per PV was determined to better understand ezetimibe-derived impact on parasite development (Fig. 2). Ezetimibe treatments markedly reduced the number of tachyzoites per meront in all three parasite species (all: $P < 0.0001$), however, the strongest effect was observed for *B. besnoiti*, with a reduction of 68.2% on the mean number of tachyzoites per meront, followed by *T. gondii* and *N. caninum* showing more than 50% reduction (56.5% and 50.2%, respectively).

Fast replicating coccidian fulfil their replication cycle within 36–48 h p. i. in BUVEC layers *in vitro* (Taubert *et al.*, 2006; Silva *et al.*, 2019; Velásquez *et al.*, 2019). In this context, the sustained inhibitory effect of ezetimibe over time was evaluated by counting tachyzoite production daily at 48, 72 and 92 h p. i. As depicted in Fig. 3, ezetimibe (20 µM) effectively blocked *T. gondii* (99.1 ± 0.0% reduction; A1–A4), *N. caninum* (75.9 ± 7.6% reduction; B1–B4) and *B. besnoiti* (99.6 ± 0.1% reduction; C1–C4) replication over time (48, 72 and 96 h p. i.).

To estimate whether ezetimibe induces either parasitostatic or parasitocidal effects, compound withdrawal experiments were performed at 24 h p. i. As illustrated in Fig. 4, remnant *T. gondii* and *N. caninum* tachyzoites quickly recovered and regained proliferative capacities 24 h after ezetimibe withdrawal. In contrast, *B. besnoiti* proved more sensitive for ezetimibe treatments showing an ongoing reduction (31.6 ± 5.3%) of tachyzoite production when compared to non-treated cells ($P = 0.15$).

Ezetimibe treatments reduce tachyzoite infectivity but fail to affect host cell permissiveness

To fulfil intracellular replication tachyzoites must first actively invade the host cells. To determine if anti-parasitic effects of ezetimibe also relied on reduced infection rates, both compartments, i. e. host cells and parasites, were separately treated with ezetimibe and then tested for infection rates 4 h after infection. Therefore, BUVEC were pre-treated with ezetimibe for 48 h before infection. At 4 h p. i. non-treated control cells presented an infection rate of 50.2% (Fig. 5A), 51.8% (Fig. 5B) and 47.0% (Fig. 5C), for *T. gondii*, *N. caninum* and *B. besnoiti*, respectively. In pre-treated cells, similar infection rates were observed for each parasite species (Fig. 5A–C), thereby denying any effect of ezetimibe pre-treatments. In contrast, ezetimibe pre-treatments of fresh tachyzoites significantly reduced invasive capacities of *T. gondii* ($P = 0.0079$; Figure 5A), *N. caninum* ($P = 0.0159$; Figure 5B) and *B. besnoiti* ($P = 0.0079$; Figure 5C) tachyzoites, when compared to non-treated control stages. Here, species-dependent effects

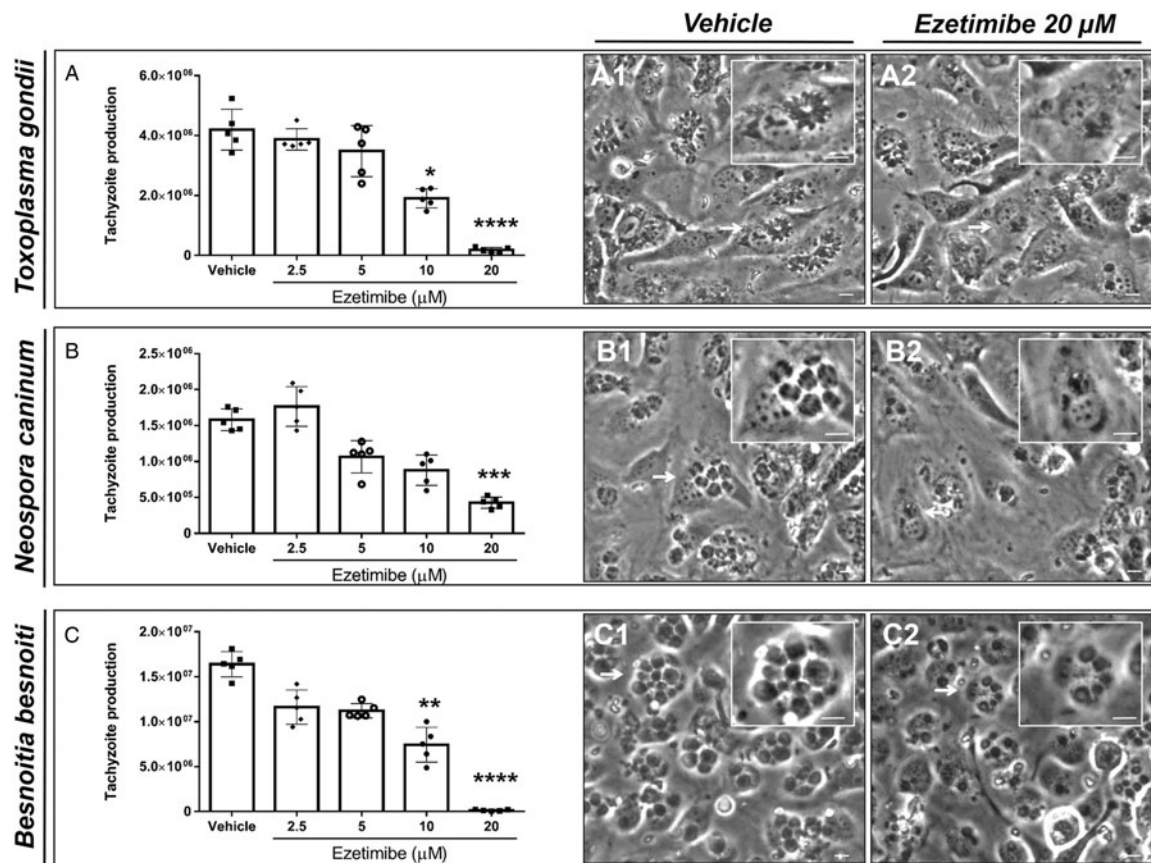


Fig. 1. Ezetimibe treatments inhibit *T. gondii*, *N. caninum* and *B. besnoiti* tachyzoite proliferation in primary endothelial cells. BUVEC were treated with ezetimibe (2.5, 5, 10 and 20 μM) 48 h before (A) *T. gondii*, (B) *N. caninum* or (C) *B. besnoiti* infection (MOI 1:5). 48 h after infection, the number of tachyzoites present in cell culture supernatants were counted (A–C). Exemplary illustration of *T. gondii* (A1–A2) *N. caninum* (B1–B2) or *B. besnoiti* (C1–C2) meront development at 24 h post infection. Scale bar represents 5 μm. Bars represent means of five biological replicates ± standard deviation. * $P \leq 0.05$; ** $P \leq 0.01$; *** $P \leq 0.001$; **** $P \leq 0.0001$.

were observed since the impact of ezetimibe pre-treatments were more prominent in case of *B. besnoiti* (28.1% reduction) than in *T. gondii* (22.2% reduction) or *N. caninum* (17.3% reduction).

Ezetimibe glucuronidation causes loss of anti-parasitic efficacy

Ezetimibe-glucuronide is the major and pharmacologically active metabolite of ezetimibe following *in vivo* liver biotransformation. Thus, a functional assay to evaluate the effect of this chemically modified molecule on tachyzoite proliferation *in vitro* was performed (Fig. 6). Here, only ezetimibe but not its glucuronated derivative led to a reduction of *T. gondii*, *N. caninum* nor *B. besnoiti* tachyzoite proliferation.

NPC1L1 gene is inconsistently transcribed in *T. gondii*, *N. caninum*- and *B. besnoiti*-infected BUVEC

Given that NPC1L1 is described as the main target of ezetimibe in humans, the profile of gene transcription of NPC1L1 was estimated over infection kinetics (3–24 h p. i.) on *T. gondii*-, *N. caninum*- and *B. besnoiti*-infected BUVEC by qRT-PCR. Using bovine small intestine tissue samples, the functionality of the qPCR system was proved. However, infection-related data showed that neither *T. gondii*-, *N. caninum*- and *B. besnoiti*-infected BUVEC nor non-infected controls have a reliable amplification of NPC1L1 mRNAs. Specifically, as illustrated in supplementary Table 1, NPC1L1 was not detected in a consistent manner, thereby showing amplification only in some of the replicates at a rather high threshold cycle (CT > 30). Consequently, no

infection-driven effect on NPC1L1 gene transcription was assumed.

Treatments does not cause cytotoxic damage to host cells or tachyzoites

To evaluate if ezetimibe (20 μ) treatment induced tachyzoite dead trypan blue exclusion test was performed. Our data showed an average viability of 95.2% ± 1.3, 90.7% ± 1.9 and 93.7% ± 2.1 for *T. gondii*, *N. caninum* and *B. besnoiti* tachyzoites treated for 1 h with vehicle control (DMSO 0.06%) without significant effects provoked by ezetimibe (Fig. S1 A–C). Moreover, the cytotoxicity of ezetimibe or ezetimibe-glucuronide on endothelial host cells XTT test was performed. As illustrated in Fig. S1 D, treatments with ezetimibe or ezetimibe-glucuronide did not induce significant colorimetric changes in the formazan product compared to the vehicle control (DMSO 0.06%).

Discussion

Cholesterol is a major component of eukaryotic cell membranes (Luo *et al.*, 2020). Given that apicomplexan parasites are generally considered as defective in cholesterol synthesis, they need to obtain this molecule from the host cell. Thus, LDL-driven cholesterol uptake is considered as a key pathway to fulfil cholesterol requirements during parasite merogony in different parasite species (Labaied *et al.*, 2011; Coppens, 2013; Ehrenman *et al.*, 2013; Hamid *et al.*, 2014; Hamid *et al.*, 2015; Nolan *et al.*, 2015; Taubert *et al.*, 2018; Silva *et al.*, 2019). Additionally, in case

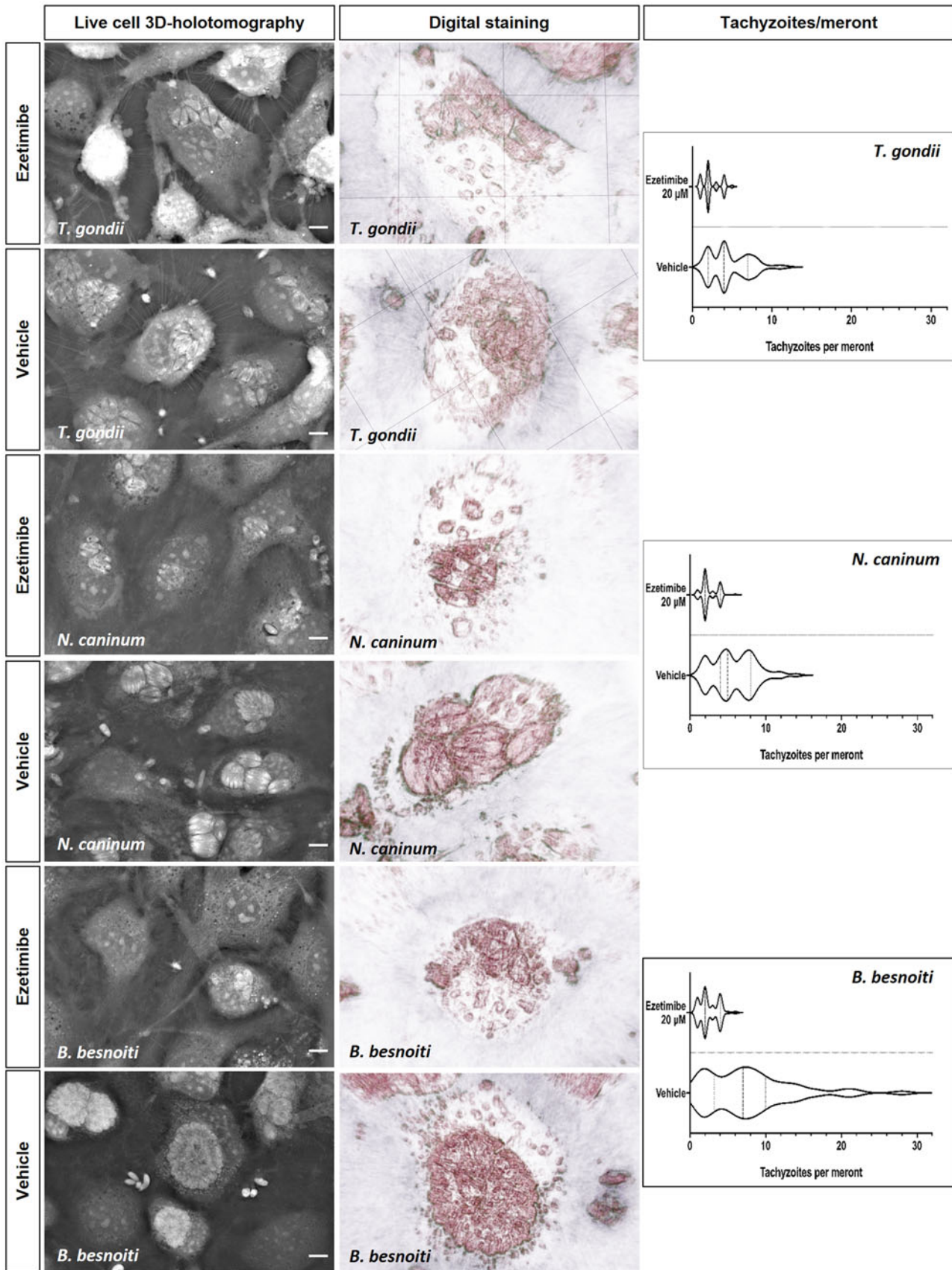


Fig. 2. Ezetimibe treatment affects intracellular meront formation and reduces the number of *T. gondii*, *N. caninum* and *B. besnoiti* intra-meront tachyzoites. Ezetimibe-pretreated BUVEC were infected with *T. gondii*, *N. caninum* and *B. besnoiti* tachyzoites and live cell 3D holotomographic microscopy was performed at 24 h p. i. Digital staining was achieved via STEVE software analysis. Violin plots depict the distribution of absolute *T. gondii*, *N. caninum* and *B. besnoiti* tachyzoite number per meront.

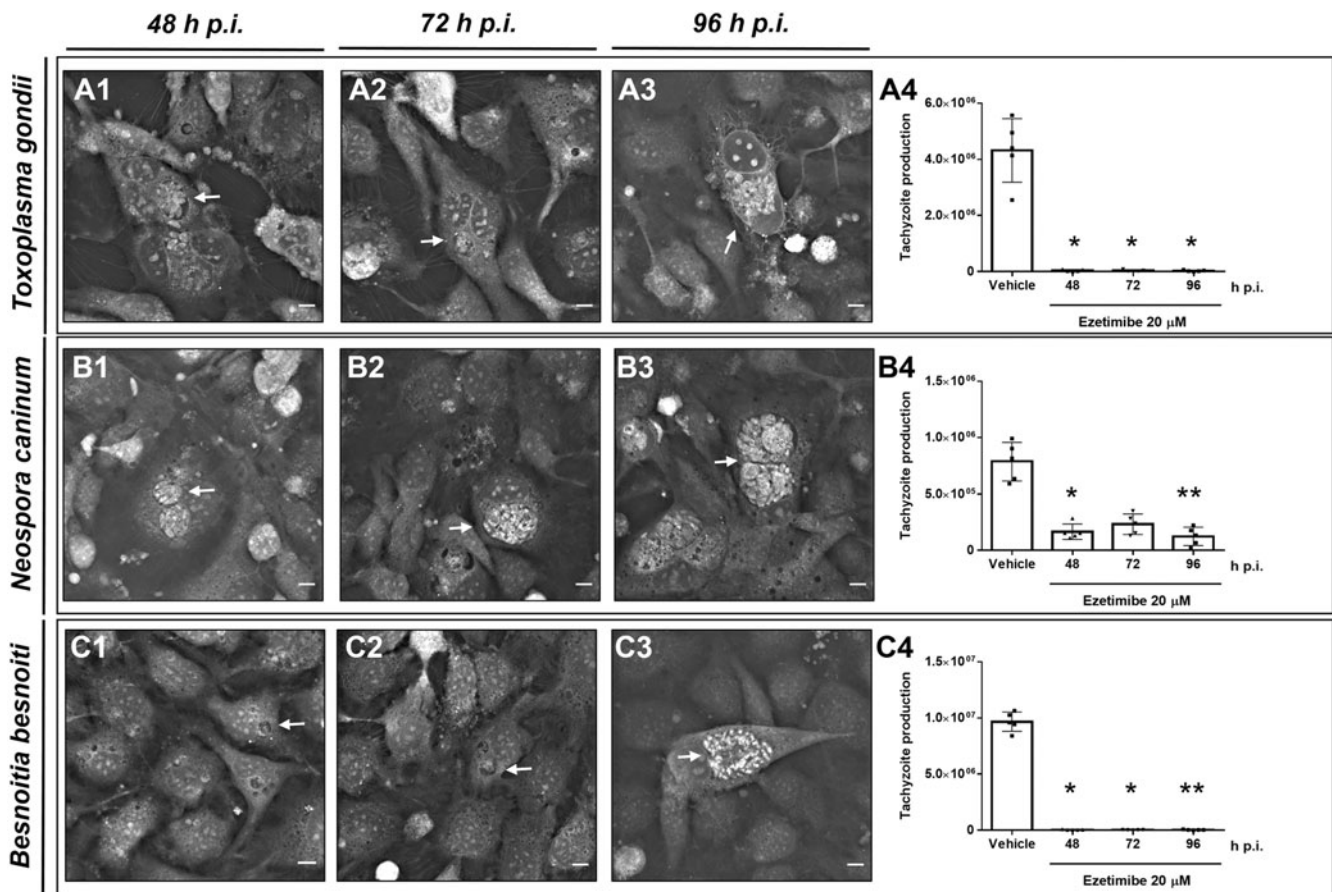


Fig. 3. Ezetimibe blocks *T. gondii*, *N. caninum* and *B. besnoiti* tachyzoite proliferation over time. Effect of daily ezetimibe treatments on tachyzoite proliferation over time: BUVEC were treated with ezetimibe (20 μ M) 48 h before infection and then infected with *T. gondii* (A), *N. caninum* (B) and *B. besnoiti* (C) tachyzoites. Exemplary live cell 3D holotomographic illustration of *T. gondii* (A1–A3), *N. caninum* (B1–B3) or *B. besnoiti* (C1–C3) meront development (arrows) at 48, 72 and 96 h p. i., respectively. At 48, 72 and 96 h p. i., the number of tachyzoites present in cell culture supernatants were counted (A4, B4, C4). Bars represent means of five biological replicates \pm standard deviation. * $P \leq 0.05$; ** $P \leq 0.01$; *** $P \leq 0.001$; **** $P \leq 0.0001$.

of *C. parvum*-infected Caco-2 cells, cholesterol is incorporated via NPC1L1-mediated micellar uptake (Ehrenman *et al.*, 2013). NPC1L1 is a trans-membrane protein highly expressed in enterocytes that mediates sterol internalization via clathrin-coated vesicles and it has widely been accepted as main target of the lipid-lowering drug ezetimibe (Altmann *et al.*, 2004; Garcia-Calvo *et al.*, 2005; Betters and Yu, 2010).

Current data demonstrate for the first time that ezetimibe has inhibitory effects on *T. gondii*, *N. caninum*, and *B. besnoiti* tachyzoite replication in primary host endothelial cells, i.e. a host cell type that is parasitized *in vivo* during the acute phase of toxoplasmosis, neosporosis and besnoitiosis (Maley *et al.*, 2003; Alvarez-Garcia *et al.*, 2013; Konradt *et al.*, 2016). Here, 10 μ M ezetimibe treatment effectively blocked *T. gondii* and *B. besnoiti* proliferation, while *N. caninum* revealed less sensitive and inhibition needed a higher concentration of 20 μ M. However, both concentrations are in range or even lie below the concentration known to block effectively NPC1L1 endocytosis (25–100 μ M, Ehrenman *et al.*, 2013). Applying 20 μ M ezetimibe as effective concentration to all species studied, the anti-parasitic effects of this compound over time were explored. Its inhibitory effect on tachyzoite proliferation was consistent over time, since the number of newly released tachyzoites at 48, 72 and 96 h p. i. was consistently low. Thus, an overall reduction of tachyzoite production of 95.7, 73.1 and 99.2% was obtained for *T. gondii*, *N. caninum* and *B. besnoiti*, respectively. These findings in principle match data from *C. parvum*-infected Caco-2 cells (permanent cell line), where a growth reduction of 65% was achieved at 25–100 μ M

concentrations (Ehrenman *et al.*, 2013). *In vitro* anti-parasitic efficacy of ezetimibe was also reported for *L. amazonensis* where 10 μ M ezetimibe reduced promastigote replication, however, amastigote production was only affected at double doses (20 μ M; Andrade-Neto *et al.*, 2016). This stage-specific discrepancy might be explained by a lower sensitivity of intracellular stages to ezetimibe treatments. Still, the concentrations here used do not necessarily support this assumption, since high effects were found at 10 μ M ezetimibe in case of *T. gondii* and *B. besnoiti*-infected BUVEC. Thus, stage- and species-related or even host cell type-related sensitivities may play a role. In line, *P. falciparum*-merozoite replication was effectively blocked only at much higher concentrations of 80 μ M ezetimibe *in vitro* (Hayakawa *et al.*, 2020).

Successful parasite offspring formation relies on several defined processes starting with active cell invasion, formation of the PV, replication and egress (Black and Boothroyd, 2000). In this context, ezetimibe pre-treated extracellular tachyzoites showed impaired infection capacities, thereby hampering the replication process at the starting point. Of note, *B. besnoiti* tachyzoites appeared more sensitive to this treatment than *T. gondii* and *N. caninum* tachyzoites, the latter of which were hardly affected in their host cell invasion capacity.

A more detailed analysis of parasite intracellular development revealed an altered morphology of meronts in the case of all three parasites in treated host cells, suggesting that prolonged ezetimibe exposition indeed affected tachyzoite physiology, thereby reducing or hampering their ability to proliferate. Residual effects of ezetimibe on *in vitro* tachyzoite replication were evaluated by drug-

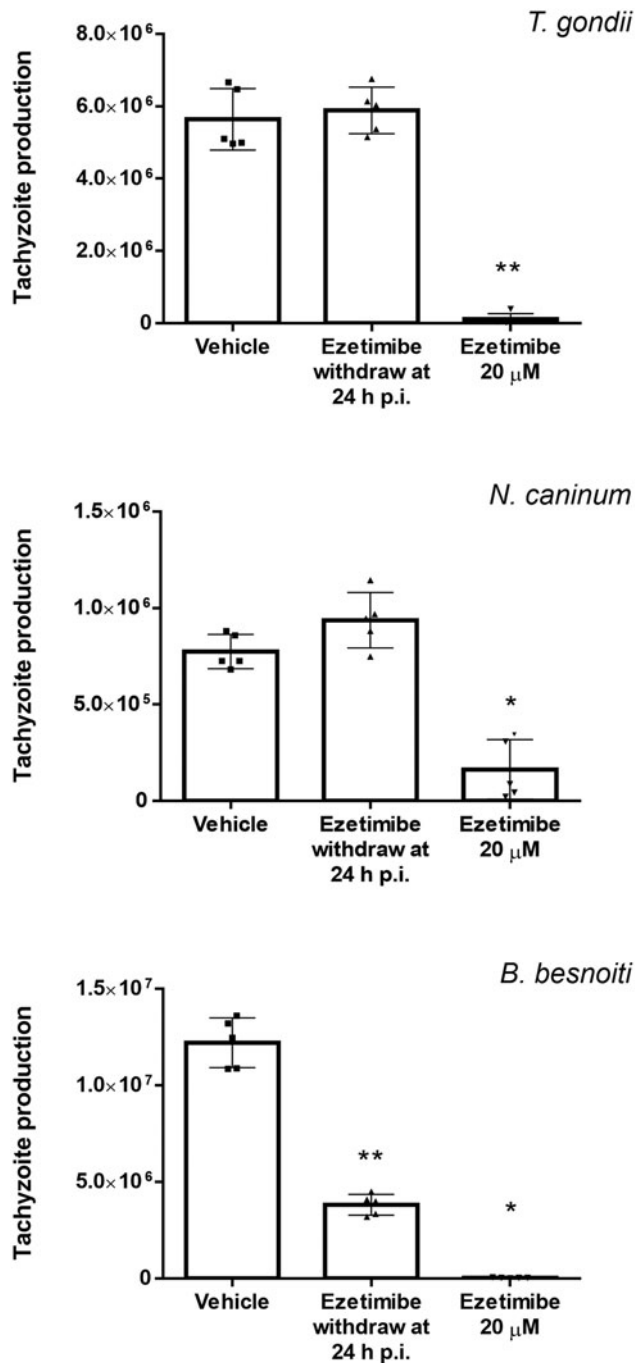


Fig. 4. Ezetimibe withdrawal restores *T. gondii* and *N. caninum* tachyzoite replication but hardly affects *B. besnoiti* recovery. Ezetimibe-treated BUVEC were infected with *T. gondii*, *N. caninum* and *B. besnoiti* tachyzoites. At 24 h p. i., ezetimibe was removed from cultures and tachyzoites present in supernatants 24 h after withdrawal were counted. Bars represent means of five biological replicates, standard deviation. * $P \leq 0.05$; ** $P \leq 0.01$; *** $P \leq 0.001$; **** $P \leq 0.0001$.

withdrawal experiments. Notably, *T. gondii* and *N. caninum* tachyzoites recovered within 24 h post withdrawal and proliferated at normal replication rates thereby showing that ezetimibe mainly induced developmental arrest but did not kill the parasites. In contrast, *B. besnoiti* tachyzoites suffered more profoundly from ezetimibe treatments since drug removal did not result in full recovery of parasite replication. These reactions indeed indicated species-specific sensitivity towards ezetimibe.

Overall, it is challenging to dissect if ezetimibe exclusively affects the parasites and/or the host cells, or if cumulative effects are to be considered. However, the current data showed that pre-

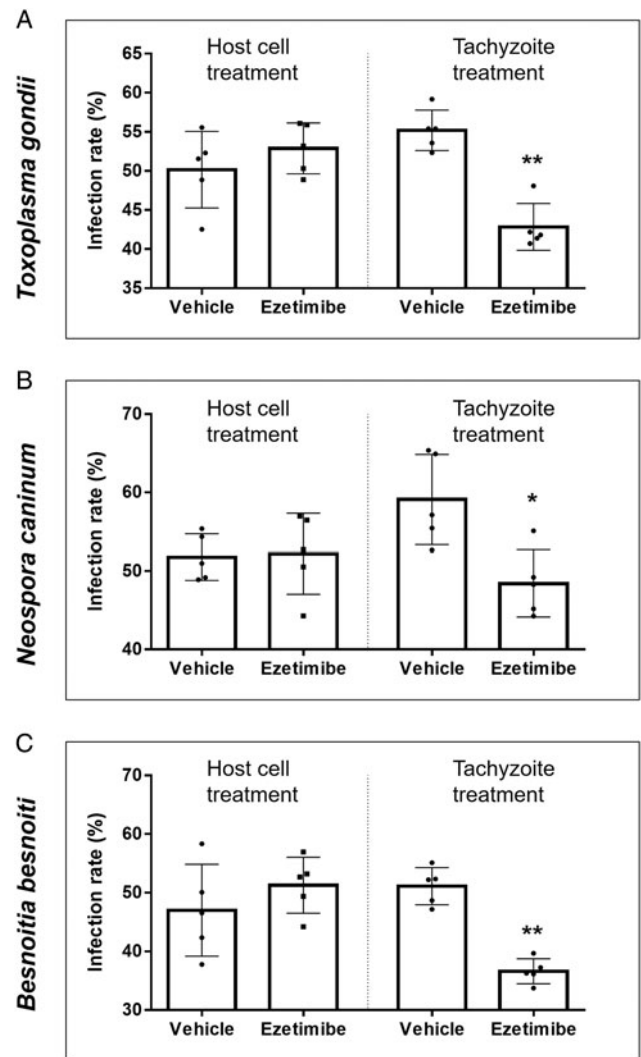


Fig. 5. Ezetimibe treatment affects the infection capacity of *T. gondii*, *N. caninum* and *B. besnoiti* tachyzoites. Non-treated or ezetimibe-treated BUVEC were infected with ezetimibe-treated or non-treated *T. gondii* (A), *N. caninum* (B) and *B. besnoiti* (C) tachyzoites. After 4 h, infection rates were estimated. Bars represent infection rate mean of five biological replicates \pm standard deviation. * $P \leq 0.05$; ** $P \leq 0.01$.

treatments of host cells did not affect infection permissiveness since infection rates were similar in treated and control cells, when using non-treated tachyzoites for infection. Nevertheless, ezetimibe treatment of tachyzoites before host cell invasion led to a significant reduction of infection rates, suggesting that ezetimibe also directly acts on tachyzoite invasive capacity in a rather species-dependent manner. Besides this mode of action, anti-parasitic activity of ezetimibe was also associated with inhibition of parasite replication within PV. By using live cell 3D holotomographic microscopy as a reliable tool for 3D cell visualization *in vivo* (Silva *et al.*, 2019; Velásquez *et al.*, 2019), we showed that ezetimibe-treated host cells infected with *T. gondii*, *N. caninum* and *B. besnoiti* presented a reduced number of tachyzoites per meront. Summarizing these data, ezetimibe might act on both, extra- and intracellular tachyzoites.

Hypolipidaemic/cholesterol-lowering properties of ezetimibe have previously been reported for humans as well as animals (Bays *et al.*, 2001; van Heek *et al.*, 2001; Knopp *et al.*, 2003). *In vivo*, this compound undergoes phase II metabolism to form a glucuronide conjugate, thereby improving NPC1L1-specific affinity and binding capacities (García-Calvo *et al.*, 2005). Besides being the major metabolite detected in plasma (García-Calvo *et al.*, 2005), ezetimibe-glucuronide is therefore

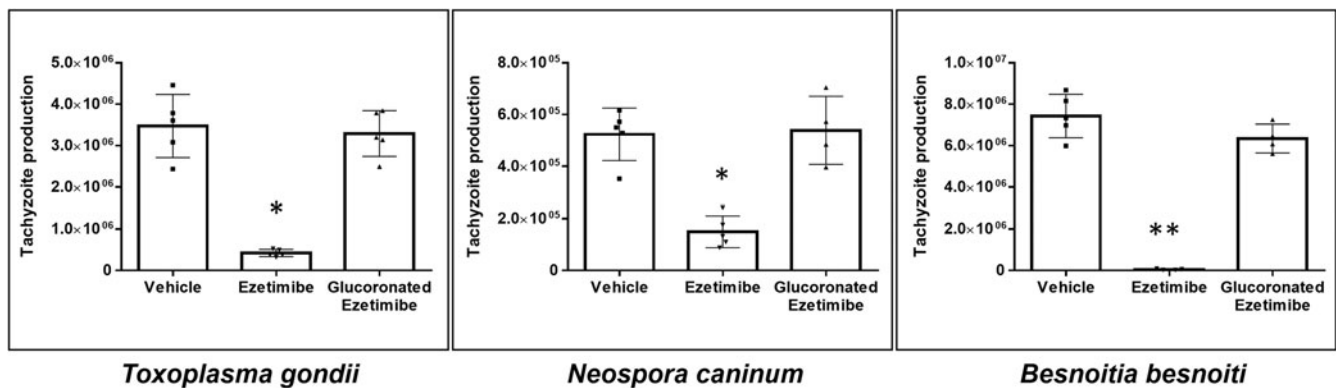


Fig. 6. Ezetimibe-mediated anti-parasitic effects are abolished by glucuronation. Ezetimibe- or ezetimibe-glucuronide-pre-treated BUVEC were infected with *T. gondii* (A), *N. caninum* (B) and *B. besnoiti* (C) tachyzoites. 48 h after infection, the number of tachyzoites present in cell culture supernatants were counted. Bars represent means of five biological replicates ± standard deviation. * $P \leq 0.05$; ** $P \leq 0.01$; *** $P \leq 0.001$; **** $P \leq 0.0001$.

considered as main active metabolite in ezetimibe treatments *in vivo*. To parallel *in vivo* situation, additional studies on the effect of ezetimibe-glucuronide on *T. gondii*, *B. besnoiti* and *N. caninum* tachyzoite proliferation *in vitro* were performed. Unexpectedly, treatments with ezetimibe-glucuronide failed to hamper intracellular tachyzoite replication thereby implicating that ezetimibe-mediated anti-parasitic effects might be NPC1L1-independent. In line, we were not able to demonstrate a consistent infection-driven induction of NPC1L1 mRNAs since these gene transcripts could hardly be detected in infected BUVEC or control cells even though intestinal control tissues gave good PCR signals. Consequently, we here assume a very low expression of this transporter in BUVEC. Likewise, the presence of NPC1L1 protein expression by Western blotting was not achieved, so far (unpublished data). Noteworthy, ezetimibe was originally identified as an ACAT II inhibitor (Clader, 2004) and therefore as acting on other potential targets besides NPC1L1. Irrespective of this, it is well documented that NPC1L1 incorporates cholesterol through an ezetimibe-sensitive pathway, however, the binding mechanism between ezetimibe and NPC1L1 remains unknown (Better and Yu, 2010). Recently, it has been reported that ezetimibe, but not ezetimibe-glucuronide, reduces the cellular content of cholesterol esters in a NPC1L1-independent manner in human monocytes, implying an inhibition of ACAT II (Orso et al., 2019). Likewise, we here propose that the current ezetimibe-mediated anti-coccidian effects may rather be linked to an inhibition of cholesterol esterification. In agreement, the importance of functional cholesterol esterification for coccidian replication was already confirmed for *T. gondii* (Sonda et al., 2001), *B. besnoiti* (Silva et al., 2019) and *E. bovis* (Hamid et al., 2014). However, the actual role of ezetimibe in cholesterol esterification and its cytosolic targets in primary bovine endothelial host cells should be further addressed in future studies. Even though *in vitro* studies have been published reporting anti-parasitic activities of ezetimibe treatments, *in vivo* evidence still needs to be addressed. Nevertheless, administration of ezetimibe to *L. amazonensis*-infected mice led to reduced parasite burden and boosted anti-leishmanial activity of ketoconazole (Andrade-Neto et al., 2016). However, given that ezetimibe treatments of *P. yoelii*-infected mice failed to affect parasitaemia (Kume et al., 2016) phylum-derived differences have to be assumed.

In conclusion, the current study shows that ezetimibe effectively inhibits *T. gondii*, *N. caninum* and *B. besnoiti* tachyzoite replication in BUVEC in a time-sustained but reversible manner. Apparently, the anti-coccidian effect of ezetimibe is associated with both impairment of tachyzoite infectivity and intracellular replication blockage. Of note, we additionally observed that

ezetimibe-glucuronide does not interfere with parasite replication thereby suggesting an NPC1L1-independent anti-parasitic mechanism.

Supplementary material. The supplementary material for this article can be found at <https://doi.org/10.1017/S0031182021000822>.

Data. All data are available in the manuscript and Supplementary data files.

Acknowledgements. The authors would like to thank Christine Henrich, Dr Christin Ritter and Hannah Salecker for their outstanding technical support. We also are very thankful to Prof. Dr A. Wehrend (Clinic for Obstetrics, Gynaecology and Andrology of Large and Small Animals, Justus Liebig University, Giessen, Germany) for the continuous supply of bovine umbilical cords. Further, we thank Oliver Bender (Ubl butcher shop, Langsdorf, Germany) for the supply of bovine small intestine samples.

Author contributions.

AT, CH, CL and LS conceived and designed the experiments. CL and LS performed the experiments. All authors performed analyses and interpretation of the data, preparation of the manuscript and approved final version of manuscript.

Financial support. CL was funded by the National Agency for Research and Development [(ANID), DOCTORADO BECAS CHILE/2017-72180349].

Conflict of interest. The authors declare there are no conflicts of interest.

Ethical standards. Not applicable

References

- Altmann SW, Davis HR Jr., Zhu LJ, Yao X, Hoos LM, Tetzloff G, Iyer SP, Maguire M, Golovko A, Zeng M, Wang L, Murgolo N and Graziano MP (2004) Niemann-Pick C1 like 1 protein is critical for intestinal cholesterol absorption. *Science (New York, N.Y.)* **303**, 1201–1204.
- Alvarez-Garcia G, Frey CF, Mora LM and Schares G (2013) A century of bovine besnoitiosis: an unknown disease re-emerging in Europe. *Trends in Parasitology* **29**, 407–415.
- Andrade-Neto VV, Cunha-Junior EF, Canto-Cavalheiro MM, Atella GC, Fernandes TA, Costa PR and Torres-Santos EC (2016) Antileishmanial activity of ezetimibe: inhibition of sterol biosynthesis, *in vitro* synergy with azoles, and efficacy in experimental cutaneous leishmaniasis. *Antimicrobial Agents and Chemotherapy* **60**, 6844–6852.
- Andrade-Neto VV, Rebello KM, Pereira TM and Torres-Santos EC (2021) Effect of itraconazole-ezetimibe-miltefosine ternary therapy in murine visceral leishmaniasis. *Antimicrobial Agents and Chemotherapy* **65**, e02676–20, /aac/65/5/AAC.02676-20.atom.
- Barter PJ and Rye KA (2016) New era of lipid-lowering drugs. *Pharmacological Reviews* **68**, 458–475.
- Bays HE, Moore PB, Dreihobl MA, Rosenblatt S, Toth PD, Dujovne CA, Knopp RH, Lipka LJ, Lebeaut AP, Yang B, Mellars LE, Cuffie-Jackson C, Veltri EP and Ezetimibe Study G (2001) Effectiveness and tolerability

- of ezetimibe in patients with primary hypercholesterolemia: pooled analysis of two phase II studies. *Clinical Therapeutics* **23**, 1209–1230.
- Benavides J, Fernandez M, Castano P, Ferreras MC, Ortega-Mora L and Perez V** (2017) Ovine toxoplasmosis: a new look at its pathogenesis. *Journal of Comparative Pathology* **157**, 34–38.
- Bettors JL and Yu L** (2010) NPC1L1 And cholesterol transport. *FEBS Letters* **584**, 2740–2747.
- Black MW and Boothroyd JC** (2000) Lytic cycle of *Toxoplasma gondii*. *Microbiology and Molecular Biology Reviews* **64**, 607–623.
- Cervantes-Valencia ME, Hermosilla C, Alcalá-Canto Y, Tapia G, Taubert A and Silva LMR** (2019) Antiparasitic efficacy of curcumin against *Besnoitia besnoiti* tachyzoites in vitro. *Frontiers in Veterinary Science* **5**, 333. doi: 10.3389/fvets.2018.00333
- Clader JW** (2004) The discovery of ezetimibe: a view from outside the receptor. *Journal of Medicinal Chemistry* **47**, 1–9.
- Coppens I** (2013) Targeting lipid biosynthesis and salvage in apicomplexan parasites for improved chemotherapies. *Nature Reviews Microbiology* **11**, 823–835.
- Davis HR Jr., Zhu LJ, Hoos LM, Tetzloff G, Maguire M, Liu J, Yao X, Iyer SP, Lam MH, Lund EG, Detmers PA, Graziano MP and Altmann SW** (2004) Niemann-Pick C1 like 1 (NPC1L1) is the intestinal phytosterol and cholesterol transporter and a key modulator of whole-body cholesterol homeostasis. *Journal of Biological Chemistry* **279**, 33586–33592.
- Ehrenman K, Wanyiri JW, Bhat N, Ward HD and Coppens I** (2013) *Cryptosporidium parvum* scavenges LDL-derived cholesterol and micellar cholesterol internalized into enterocytes. *Cellular Microbiology* **15**, 1182–1197.
- García-Calvo M, Lisnock J, Bull HG, Hawes BE, Burnett DA, Braun MP, Crona JH, Davis HR Jr., Dean DC, Detmers PA, Graziano MP, Hughes M, Macintyre DE, Ogawa A, O'Neill K A, Iyer SP, Shevell DE, Smith MM, Tang YS, Makarewicz AM, Ujjainwalla F, Altmann SW, Chapman KT and Thornberry NA** (2005) The target of ezetimibe is Niemann-Pick C1-like 1 (NPC1L1). *Proceedings of the National Academy of Sciences of the United States of America* **102**, 8132–8137.
- Ge L, Wang J, Qi W, Miao HH, Cao J, Qu YX, Li BL and Song BL** (2008) The cholesterol absorption inhibitor ezetimibe acts by blocking the sterol-induced internalization of NPC1L1. *Cell Metabolism* **7**, 508–519.
- Hamid PH, Hirtzmann J, Hermosilla C and Taubert A** (2014) Differential inhibition of host cell cholesterol de novo biosynthesis and processing abrogates *Eimeria bovis* intracellular development. *Parasitology Research* **113**, 4165–4176.
- Hamid PH, Hirtzmann J, Kerner K, Gimpl G, Lochnit G, Hermosilla CR and Taubert A** (2015) *Eimeria bovis* infection modulates endothelial host cell cholesterol metabolism for successful replication. *Veterinary Research* **46**, 100.
- Hayakawa EH, Yamaguchi K, Mori M and Nardone G** (2020) Real-time cholesterol sorting in *Plasmodium falciparum*-erythrocytes as revealed by 3D label-free imaging. *Scientific Reports* **10**, 2794.
- Hayakawa EH, Kato H, Nardone GA and Usukura J** (2021) A prospective mechanism and source of cholesterol uptake by *Plasmodium falciparum*-infected erythrocytes co-cultured with HepG2 cells. *Parasitology International* **80**, 102179.
- Knopp RH, Gitter H, Truitt T, Bays H, Manion CV, Lipka LJ, LeBeaut AP, Suresh R, Yang B, Veltri EP and Ezetimibe Study G** (2003) Effects of ezetimibe, a new cholesterol absorption inhibitor, on plasma lipids in patients with primary hypercholesterolemia. *European Heart Journal* **24**, 729–741.
- Konradt C, Ueno N, Christian DA, Delong JH, Pritchard GH, Herz J, Bzik DJ, Koshy AA, McGavern DB, Lodoen MB and Hunter CA** (2016) Endothelial cells are a replicative niche for entry of *Toxoplasma gondii* to the central nervous system. *Nature Microbiology* **1**, 16001.
- Kramer W, Girbig F, Corsiero D, Pfenninger A, Frick W, Jähne G, Rhein M, Wendler W, Lottspeich F, Hochleitner EO, Orsó E and Schmitz G** (2005) Aminopeptidase N (CD13) is a molecular target of the cholesterol absorption inhibitor ezetimibe in the enterocyte brush border membrane. *Journal of Biological Chemistry* **280**, 1306–1320.
- Kume A, Herbas MS, Shichiri M, Ishida N and Suzuki H** (2016) Effect of anti-hyperlipidemia drugs on the alpha-tocopherol concentration and their potential for murine malaria infection. *Parasitology Research* **115**, 69–75.
- Labaied M, Jayabalasingham B, Bano N, Cha SJ, Sandoval J, Guan G and Coppens I** (2011) *Plasmodium* salvages cholesterol internalized by LDL and synthesized de novo in the liver. *Cellular Microbiology* **13**, 569–586.
- Labonté ED, Howles PN, Granholm NA, Rojas JC, Davies JP, Ioannou YA and Hui DY** (2007) Class B type I scavenger receptor is responsible for the high affinity cholesterol binding activity of intestinal brush border membrane vesicles. *Biochimica et Biophysica Acta* **1771**, 1132–1139.
- Luo J, Yang H and Song B-L** (2020) Mechanisms and regulation of cholesterol homeostasis. *Nature Reviews Molecular Cell Biology* **21**, 225–245.
- Maley SW, Buxton D, Rae AG, Wright SE, Schock A, Bartley PM, Esteban-Redondo I, Swales C, Hamilton CM, Sales J and Innes EA** (2003) The pathogenesis of neosporosis in pregnant cattle: inoculation at mid-gestation. *Journal of Comparative Pathology* **129**, 186–195.
- Nayeri T, Sarvi S, Moosazadeh M, Amouei A, Hosseinijad Z and Daryani A** (2020) The global seroprevalence of anti-*Toxoplasma gondii* antibodies in women who had spontaneous abortion: a systematic review and meta-analysis. *PLoS Neglected Tropical Diseases* **14**, e0008103. doi: 10.1371/journal.pntd.0008103.
- Nolan SJ, Romano JD, Luechtefeld T and Coppens I** (2015) *Neospora caninum* recruits host cell structures to its parasitophorous vacuole and salvages lipids from organelles. *Eukaryotic Cell* **14**, 454–473.
- Orso E, Robenek H, Boettcher A, Wolf Z, Liebisch G, Kramer W and Schmitz G** (2019) Nonglucuronidated ezetimibe disrupts CD13- and CD64-coassembly in membrane microdomains and decreases cellular cholesterol content in human monocytes/macrophages. *Cytometry. Part A: The Journal of the International Society for Analytical Cytology* **95**, 869–884.
- Reichel MP, Alejandra Ayanegui-Alcérreca M, Gondim LF and Ellis JT** (2013) What is the global economic impact of *Neospora caninum* in cattle – the billion dollar question. *International Journal for Parasitology* **43**, 133–142.
- Silva LMR, Lutjohann D, Hamid P, Velásquez ZD, Kerner K, Larrazabal C, Failing K, Hermosilla C and Taubert A** (2019) *Besnoitia besnoiti* infection alters both endogenous cholesterol de novo synthesis and exogenous LDL uptake in host endothelial cells. *Scientific Reports* **9**, 6650.
- Sonda S, Ting LM, Novak S, Kim K, Maher JJ, Farese RV Jr. and Ernst JD** (2001) Cholesterol esterification by host and parasite is essential for optimal proliferation of *Toxoplasma gondii*. *Journal of Biological Chemistry*, **276**, 34434–34440.
- Taubert A, Zahner H and Hermosilla C** (2006) Dynamics of transcription of immunomodulatory genes in endothelial cells infected with different coccidian parasites. *Veterinary Parasitology* **142**, 214–222.
- Taubert A, Hermosilla C, Silva LM, Wieck A, Failing K and Mazurek S** (2016) Metabolic signatures of *Besnoitia besnoiti*-infected endothelial host cells and blockage of key metabolic pathways indicate high glycolytic and glutaminolytic needs of the parasite. *Parasitology Research* **115**, 2023–2034.
- Taubert A, Silva LMR, Velásquez ZD, Larrazabal C, Lütjohann D and Hermosilla C** (2018) Modulation of cholesterol-related sterols during *Eimeria bovis* macromeront formation and impact of selected oxysterols on parasite development. *Molecular and Biochemical Parasitology* **223**, 1–12.
- van Heek M, Farley C, Compton DS, Hoos L and Davis HR** (2001) Ezetimibe selectively inhibits intestinal cholesterol absorption in rodents in the presence and absence of exocrine pancreatic function. *British Journal of Pharmacology* **134**, 409–417.
- Velásquez ZD, Conejeros I, Larrazabal C, Kerner K, Hermosilla C and Taubert A** (2019) *Toxoplasma gondii*-induced host cellular cell cycle dysregulation is linked to chromosome missegregation and cytokinesis failure in primary endothelial host cells. *Scientific Reports* **9**, 12496.
- Velásquez ZD, Lopez-Osorio S, Pervizaj-Oruqaj L, Herold S, Hermosilla C and Taubert A** (2020) *Besnoitia besnoiti*-driven endothelial host cell cycle alteration. *Parasitology Research* **119**, 2563–2577.
- Wang J, Chu BB, Ge L, Li BL, Yan Y and Song BL** (2009) Membrane topology of human NPC1L1, a key protein in enterohepatic cholesterol absorption. *Journal of Lipid Research* **50**, 1653–1662.